Sparse aperiodic arrays for optical beam forming and LIDAR

TIN KOMLJENOVIC, ROGER HELKEY, LARRY COLDREN, AND JOHN E. BOWERS

Department of Electrical and Computer Engineering, University of California, Santa Barbara, Santa Barbara, California 93106, USA
tkomljenovic@ece.ucsb.edu

Abstract: We analyze optical phased arrays with aperiodic pitch and element-to-element spacing greater than one wavelength at channel counts exceeding hundreds of elements. We optimize the spacing between waveguides for highest side-mode suppression providing grating lobe free steering in full visible space while preserving the narrow beamwidth. Optimum waveguide placement strategies are derived and design guidelines for sparse (> 1.5 λ and > 3 λ average element spacing) optical phased arrays are given. Scaling to larger array areas by means of tiling is considered.

© 2017 Optical Society of America

References and links

1. S. J. Orfanidis, *Electromagnetic Waves and Antennas* (2016), Chap. 22.
2. W. L. Stutzman and G. A. Thiele, *Antenna Theory and Design*, 3rd ed. (Wiley, 2013), Chap. 8.
3. K. Van Acoleyen, W. Bogaerts, J. Jágerská, N. Le Thomas, R. Houdré, and R. Baets, "Off-chip beam steering with a one-dimensional optical phased array on silicon-on-insulator," Opt. Lett. **34**(9), 1477–1479 (2009).
4. J. K. Doylend, M. J. R. Heck, J. T. Bovington, J. D. Peters, L. A. Coldren, and J. E. Bowers, "Two-dimensional free-space beam steering with an optical phased array on silicon-on-insulator," Opt. Express **19**(22), 21595–21604 (2011).
5. K. Van Acoleyen, K. Komorowska, W. Bogaerts, and R. Baets, "One-dimensional off-chip beam steering and shaping using optical phased arrays on silicon-on-insulators," J. Lightwave Technol. **29**(23), 3500–3505 (2011).
6. J. K. Doylend, M. J. R. Heck, J. T. Bovington, J. D. Peters, M. L. Davenport, L. A. Coldren, and J. E. Bowers, "Hybrid III/V silicon photonic source with integrated 1D free-space beam steering," Opt. Lett. **37**(20), 4257–4259 (2012).
7. D. Kwong, A. Hosseini, J. Covey, Y. Zhang, X. Xu, H. Subbaraman, and R. T. Chen, "On-chip silicon optical phased array for two-dimensional beam steering," Opt. Lett. **39**(4), 941–944 (2014).
8. A. Yaacobi, J. Sun, M. Moresco, G. Leake, D. Coolbaugh, and M. R. Watts, "Integrated phased array for wide-angle beam steering," Opt. Lett. **39**(15), 4575–4578 (2014).
9. J. C. Hulme, J. K. Doylend, M. J. R. Heck, J. D. Peters, M. L. Davenport, J. T. Bovington, L. A. Coldren, and J. E. Bowers, "Fully integrated hybrid silicon two dimensional beam scanner," Opt. Express **23**(5), 5861–5874 (2015).
10. H. Abediasl and H. Hashemi, "Monolithic optical phased-array transceiver in a standard SOI CMOS process," Opt. Express **23**(5), 6509–6519 (2015).
11. F. Aflatouni, B. Abiri, A. Rekhi, and A. Hajimiri, "Nanophotonic projection system," Opt. Express **23**(16), 21012–21022 (2015).
12. H. Nikkhah, K. Van Acoleyen, and R. Baets, "Beam steering for wireless optical links based on an optical phased array in silicon," Ann. Telecommun. **68**(1), 57–62 (2013).
13. J. Sun, E. Hosseini, A. Yaacobi, D. B. Cole, G. Leake, D. Coolbaugh, and M. R. Watts, "Two-dimensional apodized silicon photonic phased arrays," Opt. Lett. **39**(2), 367–370 (2014).
14. J. Sun, E. Timurdogan, A. Yaacobi, E. S. Hosseini, and M. R. Watts, "Large-scale nanophotonic phased array," Nature **493**(7431), 195–199 (2013).
15. J. Sun, E. Timurdogan, A. Yaacobi, Z. Su, E. S. Hosseini, D. B. Cole, and M. R. Watts, "Large-scale silicon photonic circuits for optical phased arrays," IEEE J. Sel. Top. Quantum Electron. **20**(4), 8201115 (2014).
16. K. Van Acoleyen, H. Rogier, and R. Baets, "Two-dimensional optical phased array antenna on silicon-on-insulator," Opt. Express **18**(13), 13655–13660 (2010).
17. W. Guo, P. R. A. Binetti, M. L. Masanovic, L. A. Johansson, and L. A. Coldren, "Large-scale InP photonic integrated circuit packaged with ball grid array for 2D optical beam steering," in *IEEE Photonics Conference* (IEEE, 2013), pp. 651–652.

18. K. Sayyah, O. Efimov, P. Patterson, J. Schaffner, C. White, J.-F. Seurin, G. Xu, and A. Miglo, "Two-dimensional pseudo-random optical phased array based on tandem optical injection locking of vertical cavity surface emitting lasers," Opt. Express **23**(15), 19405–19416 (2015).
19. D. Kwong, A. Hosseini, Y. Zhang, and R. T. Chen, "1× 12 unequally spaced waveguide array for actively tuned optical phased array on a silicon nanomembrane," Appl. Phys. Lett. **99**(5), 051104 (2011).
20. J. K. Doylend, M. J. R. Heck, J. T. Bovington, J. D. Peters, and J. E. Bowers, "Free-space beam steering using silicon waveguide surface gratings," in *IEEE Photonic Society 24th Annual Meeting* (IEEE, 2011), pp. 547–548.
21. D. N. Hutchison, J. Sun, J. K. Doylend, R. Kumar, J. Heck, W. Kim, C. T. Phare, A. Feshali, and H. Rong, "High-resolution aliasing-free optical beam steering," Optica **3**(8), 887–890 (2016).
22. C. V. Poulton, M. J. Byrd, M. Raval, Z. Su, N. Li, E. Timurdogan, D. Coolbaugh, D. Vermeulen, and M. R. Watts, "Large-scale silicon nitride nanophotonic phased arrays at infrared and visible wavelengths," Opt. Lett. **42**(1), 21–24 (2017).
23. W. Song, R. Gatdula, S. Abbaslou, M. Lu, A. Stein, W. Y.-C. Lai, J. Provine, R. F. Pease, D. N. Christodoulides, and W. Jiang, "High-density waveguide superlattices with low crosstalk," Nat. Commun. **6**, 7027 (2015).
24. A. Khavasi, L. Chrostowski, Z. Lu, and R. Bojko, "Significant crosstalk reduction using all-dielectric CMOS-compatible metamaterials," IEEE Photonics Technol. Lett. **28**(24), 2787–2790 (2016).
25. H. Unz, "Linear arrays with arbitrarily distributed elements," IRE Trans. Ant. Prop. **8**(2), 222–223 (1960).
26. M. G. Bray, D. H. Werner, D. W. Boeringer, and D. W. Machuga, "Optimization of thinned aperiodic linear phased arrays using genetic algorithms to reduce grating lobes during scanning," IEEE Trans. Antenn. Propag. **50**(12), 1732–1742 (2002).
27. D. D. King, R. F. Paackard, and R. K. Thomas, "Unequally-spaced, broad-band antenna arrays," IRE Trans. Antennas Propag. **8**(4), 380–384 (1960).
28. J. Kennedy and R. Eberhart, "Particle swarm optimization," in *Proceedings of IEEE International Conference on Neural Networks IV* (IEEE, 1995), pp. 1942–1948.
29. C. V. Poulton, A. Yaccobi, Z. Su, M. J. Byrd, and M. R. Watts, "Optical phased array with small spot size, high steering range and grouped cascaded phase shifters," in *Advanced Photonics 2016* (2016), paper IW1B.2.

1. Introduction

Free-space beam-steering is important for light detection and ranging (LIDAR), free space communications, and has potential applications for holographic displays and biomedical imaging. The beam can be steered mechanically, but an optical phased array (OPA) offers many advantages such as reduced size and weight as well as increased speed due to lack of inertia. Furthermore, OPAs can, for example, be integrated with all the other required circuitry to make a fully-integrated chip-scale LIDAR system.

Phased antenna arrays have extensively been studied in radio frequencies, and there are many book chapters written about them, e.g [1,2]. OPAs, on the other hand, have received less attention, but in recent years, there has been a lot of interest in research and development of OPAs [3–22]. One of the reasons is the use of silicon photonics, with its superior processing and yield, allowing for more complex photonic integrated circuits (PIC) with hundreds or thousands of elements.

There are some key differences between phased antennas in RF and OPAs mainly due to the many orders difference in wavelength. RF arrays typically operate in centimeter wavelength range with a push to millimeter wavelength range, while OPAs operate in micrometer range, most often around 1.5 μm. It is well known that a uniform spaced array has to have the spacing between elements $d < \lambda/2$, where λ is the free-space wavelength, to prevent appearance of grating sidelobes as the main lobe is scanned across the visible region [1,2]. Depending on the scan angle range of the OPA, the limitation can be relaxed a bit, but in all cases $d < \lambda$ holds. This requirement can readily be met in RF, with some consideration due to potential unwanted cross-coupling between antenna elements. In optics the cross-coupling presents more serious challenges, with some suggestions on how to achieve sub-wavelength spacing [23,24], but that is just one of the problems in realizing such a narrow pitch that we turn to in Section 2. Each element also has to have phase control and be electrically contacted for operation, so having a lower number of elements covering the same area makes the driving circuitry simpler. Non-uniform or aperiodic arrays have been studied in 1960s [25], and they make a tradeoff in suppressing the grating lobes for an increase of power in sidelobes. As they cover the same area, the main lobe width is preserved provided that the excitation amplitude has the same taper, while control and circuitry are simplified due

to lower number of elements. Such an approach has recently been demonstrated with a larger waveguide count and has allowed for 80° steering in phase direction [21] with over 500 resolvable spots with a small divergence of 0.14°. The array had 128 emitters with average spacing of 7.245 μm at 1.3 μm or 5.57 λ. The positions were randomized using uniformly distributed random numbers and an iterative algorithm to place the waveguides so the array had > 10 dB sidemode suppression ratio (SMSR) at ± 45° deflection. The minimum pitch was set at 5.4 μm and in the final design, the standard deviation of 1.1 μm was reported.

Here our analysis goes several steps further, by first studying non-uniform ordered distributed waveguides and then various randomization approaches. We study the effect of increasing the waveguide count on key performance metrics that include the SMSR, power in the main beam and the main beam full width at half maximum (FWHM), where for randomized approaches, we utilize a global optimization technique. Power in the main beam, as reported in this manuscript, is the integrated power in the direction of the main lobe between first nulls (sometimes called null-to-null beamwidth) divided by the total radiated power of the array.

We show that normal and uniform distributions are not optimal, and also that even better performance can be obtained by using a fully random waveguide placement compared to the offset approach that was typically used to optimize thinned or aperiodic arrays [26].

The OPA design that we study is shown in Fig. 1 and is similar in operation to the ones reported in [9,21] where phase control is used to steer only in one of the axis, while the other axis is steered by wavelength. Such an approach has a distinct advantage compared to a purely phase steered 2D array due to significant reduction in number of controls required. An OPA as shown in Fig. 1 needs only $N + 1$ controls (N phases and 1 wavelength) compared to NxM controls needed for 2D phase array. As we steer the beam using phase only in one axis, our analysis is also simplified as we effectively study 1D phased arrays.
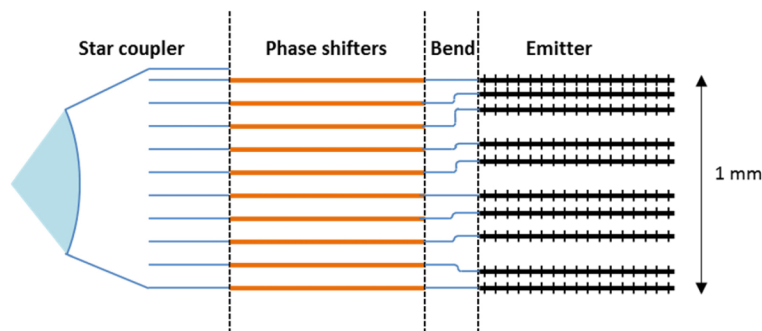

Fig. 1. Optical phase array (OPA) as studied comprises of a star coupler (splitting the input wave into N waveguides), N phase shifters, bend structures to offset the emitter positions and N emitters with non-uniform pitch. For analysis purposes we set the width of the emitter region to 1 mm throughout the manuscript, if not specified differently. This makes it ~645 λ wide at 1.55 μm.

The paper is organized as follows. In Section 2 we analyze a uniform phased array as a metric to compare the aperiodic arrays to. We also address the waveguide crosstalk, and the problem of having phase shifters at small pitch. In Section 3 we describe our method of analysis; briefly the global search algorithm employed and then study various waveguide placement strategies including ordered non-uniform pitch and fully random non-uniform pitch. In Section 4 we compare in detail two most promising placement strategies from previous section and we also address the potential for scaling to larger OPA widths using tiling of basic elements. Finally, we draw conclusions in Section 5.

2. Uniformly spaced arrays

An array of antennas can synthesize any radiation pattern, provided that it has enough elements and that they are spaced by $d < \lambda/2$. The relative displacements of the antenna elements introduce relative phase shifts in the radiation vectors, and fields from individual antennas add constructively or destructively in different directions. This is a direct consequence of the translational phase-shift property of Fourier transforms [1]. By introducing phase control into each element, the array can be steered and the angle can be scanned.

Uniformly-spaced one-dimensional arrays are probably the easiest to analyze with closed expressions derived for the array factor if the excitation is also uniform (in magnitude). In the case $d > \lambda/2$, grating lobes can appear with uniform-spaced arrays. In most cases, including the OPAs, grating lobes are undesirable, which puts severe constraints on OPA design. The angles of other grating lobes are given by

$$\sin \theta_n = \frac{n\lambda}{d} + \sin \theta_0 \qquad (1)$$

where θ_n is the angle of the n-th order grating lobe, n is the order of the grating lobe, and θ_0 is the angle of the primary beam (zeroth grating lobe).
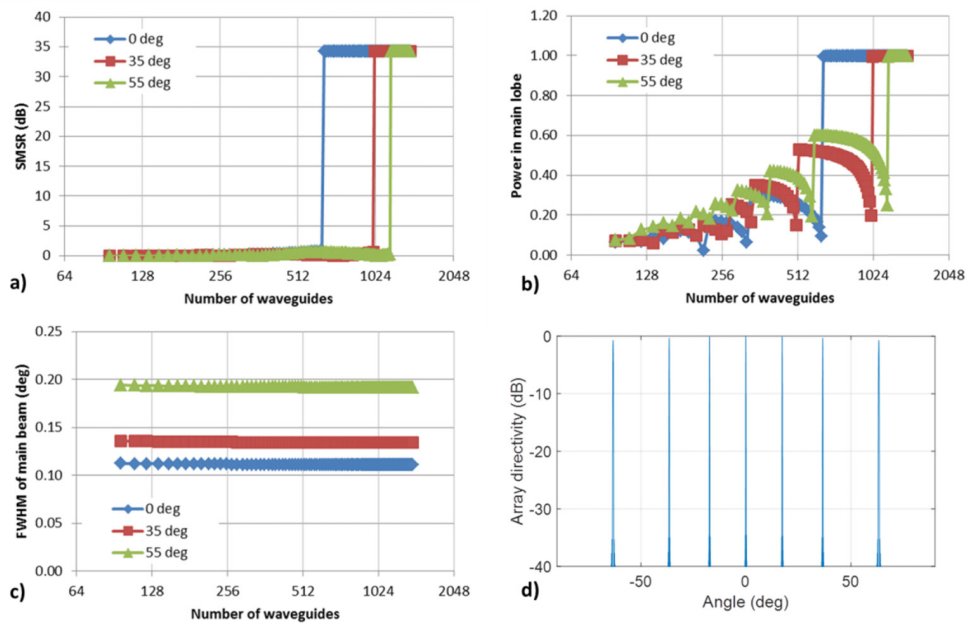

Fig. 2. (a) SMSR as a function of the number of waveguides for 1 mm wide uniformly spaced OPA. The pitch has to be reduced, so all grating lobes are pushed outside the visible region, for SMSR to improve. (b) Power in the main lobe as a function of number of waveguides for the same OPA. Power increases as grating lobe number is reduced (c) FWHM of the main beam as a function of number of waveguides. The FWHM is the same regardless of the number of waveguides, provided that the total size of the array is kept the same. (d) Illustrative far-field for an array with 192 uniformly spaced elements resulting with seven lobes in visible space when looking at broadside.

We plot the SMSR, power and FWHM of the main beam for a uniformly-spaced array 1 mm wide as a function of number of waveguides in Fig. 2. The operating wavelength is set at 1.55 μm. We taper the amplitude of the excitation to −10dB at the ends of the array to suppress the close-in sidelobes that would otherwise limit the SMSR to ~13 dB in a uniformly

excited array [1]. This lifts the SMSR limitation to ~35 dB. In all cases, unless specified otherwise, we assume that the elementary emitter has a Gaussian near-field profile with 10 dB taper at ± 250 nm (500 nm total width).

Figure 2(a) shows the SMSR as a function of the number of waveguides, or inversely as the pitch (d) is reduced. For broadside direction (0° in our notation), the grating lobes are suppressed when the waveguide count exceeds 648, or $d \approx 1.54$ μm $< \lambda$. But as the same array is steered to 35° or 55° degrees the grating lobes appear as also indicated by Eq. (1) with the right side sine term. To cover ± 35°, ± 55°, or ± 90° with no grating lobes 1018, 1176 or 1291 waveguides are needed corresponding to 0.98 μm, 0.85 μm or 0.774 μm pitch, respectively. Such small spacing is very challenging and we address it in more detail in following section. Figure 2(b) shows the relative power in the main lobe calculated as integrated power in the main lobe (null-to-null beamwidth) divided by the total radiated power. The step increases in power correspond to the reduction of number of grating lobes in visible space. In between these steps, there is a reduction of power in the main lobe due to the broadening of the grating lobes as they are steered closer to the edge of the visible region. This effect can be suppressed with a more directive elementary emitter [1]. Figure 3(c) shows the FWHM of the main lobe, and there is a key takeaway that the FWHM is not dependent on the number of waveguides if they cover the same area. The difference between FWHM for different scan directions is a direct result of reducing the effective area of the emitter array as the beam is scanned from the broadside. Figure 2(d) shows an illustrative far-field for an array with 192 uniformly spaced elements resulting with seven lobes in visible space when looking at broadside.

One could argue that e.g. the 192 waveguide configuration (5.21 μm pitch) can be used to steer the beam in ± 8.5° range as grating lobes are spaced by ~17°, but spurious signals from the grating lobes have to be suppressed for reliable measurements or there will be ambiguity in signal. For that reason, in most practical cases with uniform arrays the pitch has to be reduced to $< \lambda$ resulting in a number of challenges that have to be addressed such as crosstalk, placement and contacting the phase shifters, etc.
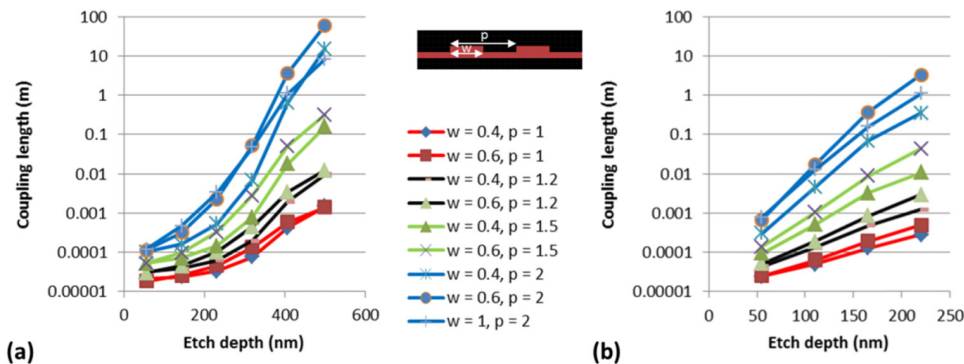

Fig. 3. Coupling length at 1.55 μm calculated by the difference in effective index of refraction between even and odd mode as a function of etch depth for different waveguide widths (w) and waveguide pitch (p). (a) 500 nm thick Si device layer (b) 220 nm thick Si device layer.

2.1 Crosstalk

Optical cross talk is a severe issue with OPAs due to the use of dielectric waveguides where it is hard to tightly confine electromagnetic waves compared to RF frequencies where metals are typically used. Use of high index contrast waveguides such as Si/SiO_2 helps, but obtaining sub-wavelength pitch without crosstalk is still very challenging. We calculate crosstalk in two standard Si photonic platforms: 220 nm thick Si device layer typically used for passive devices and thicker 500 nm Si device layer typically used for heterogeneously integrated silicon photonic devices at 1.55 μm. In both cases we calculate the coupling length

corresponding to 100% power transfer between the two straight waveguides. We study a number of pitch (waveguide spacing) values p and a few waveguide widths w, and plot the coupling length as a function of etch depth, from a very shallow to fully etched. The results are plotted in Fig. 3.

For obtaining a narrow beam in the wavelength steered dimension, one generally wants to have a long and weak grating, so the effective aperture length is large. Due to the requirement to have substantially different phases in neighboring waveguides at certain steer angles, the cross talk has to be minimized. The criterion for the amount of coupling that can be tolerated is somewhat arbitrary, and here we set the requirement for the coupling length to be 10x the grating length. In our considered case of 1 mm long grating, the coupling length has to be at least 1 cm.

From Fig. 3 it is clear that this limits us to 1.5 μm pitch with 220 nm thick silicon and to 1.2 μm pitch with 500 nm thick silicon, and generally requires full etch. In the former case, the pitch requirement allows us to suppress the grating lobes at broadside, but with practically no steering range without grating lobes, while in the latter case we have ~(± 17°) of steering without grating lobes.

There has been an effort to reduce the crosstalk between closely spaced waveguides. One way would be to introduce a phase mismatch in neighboring waveguides [23], but such an approach requires at least two corrections for optimal beam quality. First the pitch of the grating has to be corrected to account for the change in effective index of refraction (wavelength steering direction). Second, the phase has to be adjusted between the waveguides for phase steering direction. It is relatively straightforward to correct for the phase difference at one particular point, but as the emission is continuous along the grating, it is not possible to do so with a small change in feeding waveguides (either their length or their phase velocity). It seems that there have to be multiple transitions between beta values along the length of the grating so that the phase difference between neighboring waveguides does not exceed some predetermined value, making this approach quite complex. Another way of reducing the crosstalk would be the introduction of sub-wavelength periodic structures as in [24], but although the increase in coupling length is substantial, it still does not allow for 1 mm long gratings with negligible coupling and large field of view (FOV). To conclude, although there has been considerable progress, low crosstalk $\lambda/2$ pitch at 1.55 μm with compensated phase difference is still very challenging, so the ability to use larger waveguide spacing for OPAs would simplify the design and manufacturing.

2.2 Phase shifters

An ideal OPA has to have a phase shifter for every waveguide with grating. Due to the complexity of electrically connecting the phase shifters and having large enough separation between the metal and the optical field to reduce the propagation loss, they would usually have much larger pitch than the gratings (e.g. see Fig. 1 in [9] or Fig. 1 in [21]), so in the final chip the grating would occupy relatively small area increasing the cost of the OPA compared to beam width that is predominantly determined by the effective area of the gratings. From that perspective the use of larger pitch sizes would prove beneficial. Another issue with having large emitters with sub-wavelength pitch is the sheer number of phase shifters that have to be controlled increasing the system complexity, power consumption and reducing the yield.

3. Aperiodic arrays

Linear RF arrays with arbitrarily distributed elements were studied in 1960s [25], and the main motivation was that the variable spacing generally allows for fewer elements with similar far field pattern performance. The main advantages of unequally-spaced arrays are [27]: fewer elements for comparable beamwidth and grating lobe replacement by sidelobes of unequal amplitude, which are all less than the main lobe. The reduction in the number of

elements allows the arrays to be built at lower cost with lower number of amplifiers and phase shifters.

As the aperiodic array is a quite complex non-linear problem, lack of computational resources in 1960s prevented numerical optimization of such arrays, so most studied arrays had an order where spacing would follow some law: logarithmic, prime number, power spacing, while the minimum pitch would often correspond to $\lambda/2$. The increase in computational power in recent years, allowed for the far-field pattern optimization using iterative search algorithms [21, 26]. Usually global search algorithms have been used, such as genetic algorithm [26] or particle swarm optimization (PSO) [28]. Here, for randomized waveguide placement studied in Section 3.2, we employ the PSO as implemented in Matlab (R2016a) for simplicity. The calculation of non-uniform spaced array pattern (AP) is implemented in matrix notation, which is multithreaded in Matlab and reasonably fast allowing for use of a global optimization algorithm (~50 ms for calculating 192 element far field pattern in 10001 points on a modern PC). As an optimization parameter, we use the SMSR with the beam pointing in given direction.

For a typical optimization run, we used 400 particles and let the optimizer work for 1 hour. Due to the number of degrees of freedom (corresponding to number of waveguides), it is reasonable to expect that the optimizer will not find the optimal result, especially for larger waveguide counts, but with repeated optimizations we generally get less than 1 dB difference in SMSR indicating that we are relatively close to the optimal solution. Optimization of the phase of each emitter could also be implemented, but it is obvious that for the highest power in the main lobe, the phases should be aligned at the direction where the main beam points. A brief study in phase optimization showed that it is possible to improve the SMSR somewhat in certain configurations, but with severe reduction of power in the main beam, which does not seem a worthwhile route for OPAs. For that reason, when steering the non-uniform arrays, we calculate the steering phase using the well-known expression [1] $\psi = kd_i \cos(\varphi)$, where d_i is the distance of the i-th element from the array origin.

For waveguide placement, we consider both the ordered non-uniform spacing and fully random OPAs. In all cases, we impose a minimum pitch that puts some limitations on the waveguide placement. First we turn to the ordered non-uniform spacing OPAs.
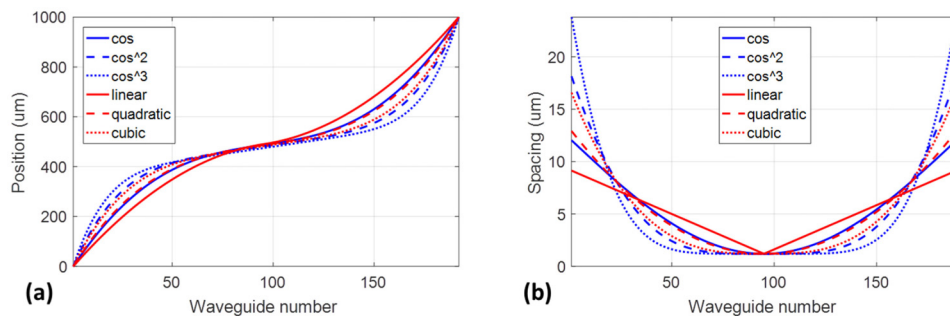

Fig. 4. (a) Position and (b) Spacing for an ordered non-uniform spacing OPAs consisting of 192 waveguides. Shown are linear, quadratic, cubic, cos, cos^2 and cos^3 spacing distribution and waveguide position. The minimum pitch is set at 1.2 μm due to cross-coupling limitations.

3.1 Ordered non-uniform spacing

There are a number of functions that we could use to determine the spacing of the ordered non-uniform spacing OPAs. We plot positions and spacings for six different functions in Fig. 4 as an illustration for the 192 waveguide case with 1.2 μm minimum pitch. We intentionally plot the case with a relatively small number of waveguides as changes between functions are more apparent.
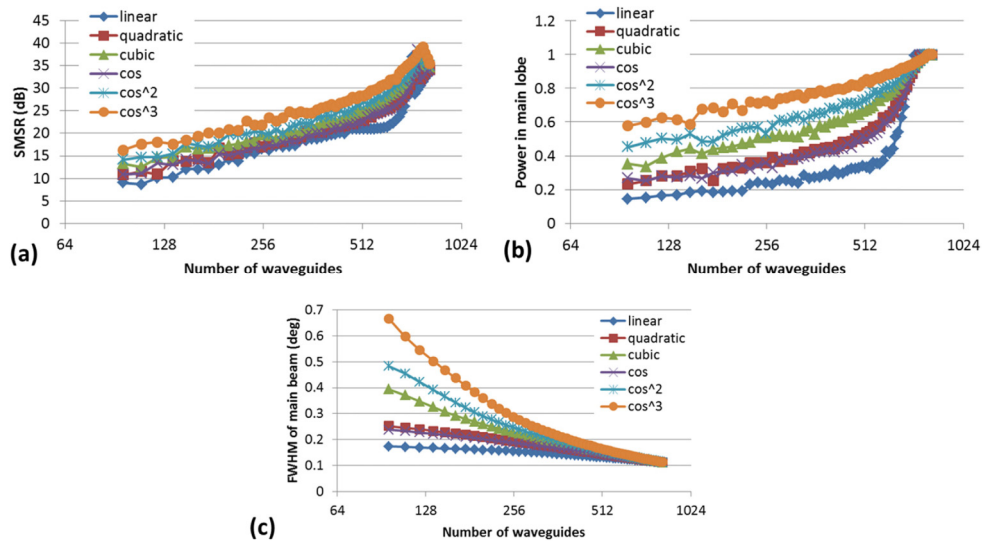
Fig. 5. (a) SMSR at broadside as a function of number of waveguides for 1 mm wide OPA with different spacing distributions. The SMSR generally improves as the number of waveguides is increase. (b) Power in the main lobe at broadside as a function of number of waveguides for the same OPA. Power increases as number of waveguides is increased (c) FWHM of the main beam at broadside as a function of number of waveguides. The FWHM reduces with increase of number of waveguides contrary to the uniform case.

Similar to the uniform pitch case (Fig. 2), we plot the SMSR, power in main lobe and FWHM as a function of the number of waveguides. We limit the number of considered waveguides to 820 due to minimum pitch requirement of 1.2 μm. The results are plotted in Fig. 5. One could conclude, looking at Fig. 5, that the cos^3 spacing distribution is superior due to highest SMSR and power in the main lobe, with the tradeoff being wider main lobe, but that conclusion is valid only at broadside.

Next we study the beam steering performance. Due to constraints placed by the minimum pitch (1.2 μm in this case due to cross-coupling, see Section 2.1) and the total number of waveguides, there is not much difference between some functions (e.g. cos and quadratic), so, due to space consideration, we show results only for linear, quadratic, and cos^3 in more detail as we steer the beam. We study cases with 192 and 480 waveguides, both of which are much smaller than the 1300 waveguides needed for uniform pitch with no grating sidelobes for a 1 mm wide emitter. We plot the SMSR, power in main lobe and FWHM as a function of steering angle in Fig. 6. It is again clear that the more squeezed the waveguides are (e.g. cos^3) we have better SMSR and more power in main lobe, at the expense of the FWHM, but that holds only for smaller steer angles. As we steer more, the SMSR for such squeezed spacings deteriorates rapidly as the large grating lobe that is not strongly suppressed comes into the visible region. A linear change of pitch, on the other hand, has worse SMSR and power in main lobe at broadside, but the performance is largely unaffected by steering the beam, so it is probably preferred for large FOV applications. Non-uniform ordered spacing, as the one considered here, in all cases trades off the FWHM and the quality of the main beam for SMSR. Wider FWHM of the main beam results with more power in the main beam, which helps with range in the case of LIDAR application. At the same time, it influences the number of resolvable spots. The number of resolvable spots with > 10 dB SMSR is much larger with linear and quadratic spacings due to the much larger FOV and narrower lobe compared to cos^3 spacing (approximately 600-700 vs. only 75 in case of 480 waveguides).
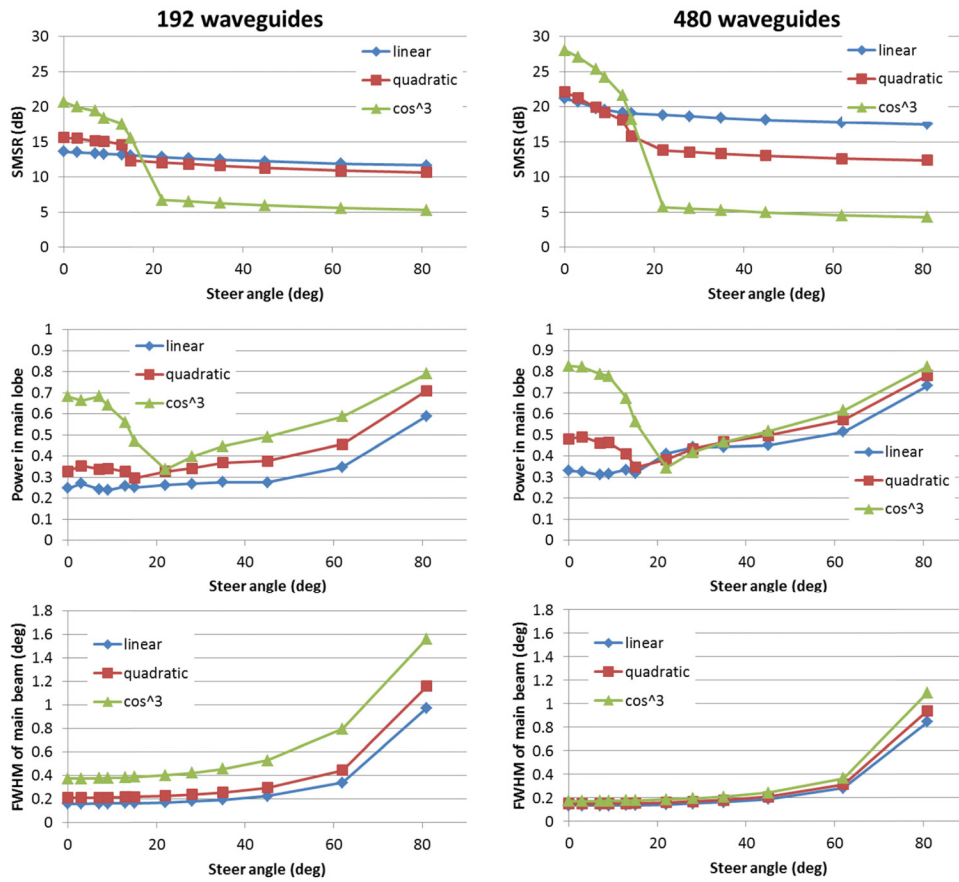
Fig. 6. SMSR, power in main lobe and FWHM of the main lobe as a function of steer angle for ordered non-uniform OPAs with linear, quadratic and cos^3 spacing distributions. (left column) 192 waveguide configuration (right column) 480 waveguide configuration.

Finally, we study the influence of minimum pitch on the OPA performance. Due to space constraints, we show only results for linear and cos^3 non-uniform spacing OPAs as two extreme configurations in Fig. 7. It is clear that for cos^3, a small minimum pitch is required with performance quickly deteriorating as the pitch is increased to ~λ scale, linear pitch is on the contrast largely insensitive to minimum pitch, especially at lower waveguide counts.

Once again we can conclude that linear change in pitch is better if wide FOV is required, while more compressed schemes (quadratic, cubic, cos^3, etc.) can be used for limited FOV if sub-wavelength pitch can be attained as they can offer higher SMSR and higher power in the main lobe. It should be pointed out that linear change in pitch offers decent performance with 192 waveguides even with minimum pitch in 3 μm range (~2 λ) where crosstalk can definitely be neglected.
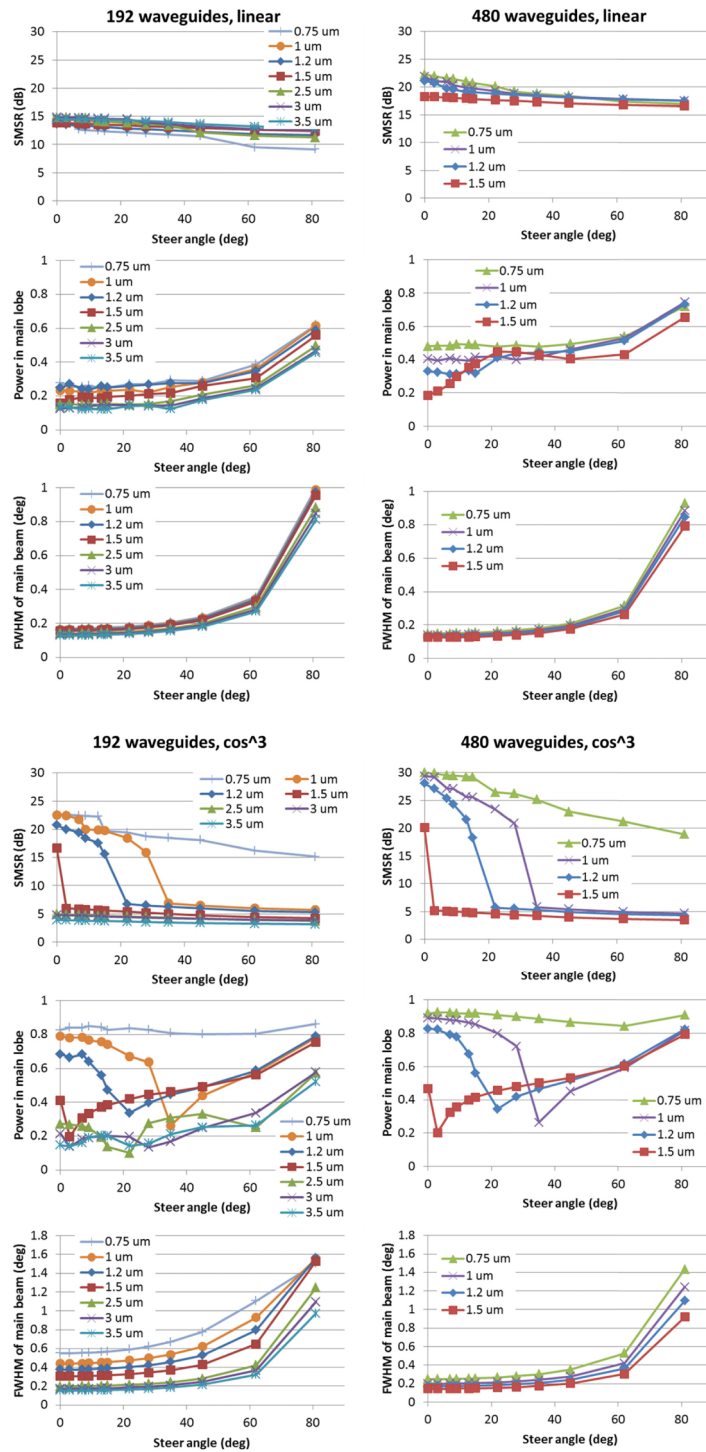
Fig. 7. SMSR, power in main lobe and FWHM of the main lobe as a function of steer angle for ordered non-uniform OPAs with linear and cos^3 spacing distributions for different minimum pitch with 192 and 480 waveguides.

3.2 Randomized non-uniform spacing

We now turn to the analysis of randomized non-uniform spacing using the PSO algorithm to determine optimal spacing. First we compare the randomization approaches, from truly random distributions (both normal and uniformly distributed offsets), PSO optimized offset spacing similar to [26] and fully random PSO distribution. For truly random distributions, we generate a uniform pitch and then a sequence of random numbers with normal or uniform distribution. We then offset the uniform waveguide positions using those generated sequences. As it is a purely random approach sensitive to "roll of dice", we repeat the process three times and average the result that we plot in Fig. 8. For the PSO optimized offset spacing, we utilize an approach similar to one outlined in [26] where we initially position the waveguides at uniform pitch and then adjust the offsets from the uniform pitch keeping the minimum spacing requirement satisfied using the PSO algorithm. In this case the offset is limited to (average pitch – minimum pitch)/2. Lastly we implement a fully random spacing, in which we skip the generation of the uniform array and add element by element to a location where the distance between the last element is greater than minimum pitch and is less than the distance needed to place all remaining elements at minimum pitch and is further scaled by the random value for that element divided by the sum of the unused part of the random vector. This approach allows us to shuffle the waveguide positions more while still keeping the minimum pitch requirement satisfied. The comparison between all the approaches as a function of number of waveguides is shown in Fig. 8. In Fig. 9 we show histograms with typical offsets from the uniform pitch for the case of 480 waveguides for different waveguide placement strategies. The minimum pitch is 1.2 μm in all cases. The added freedom of the fully random approach allows the optimizer to suppress the sidelobes with 480 and 576 waveguides compared to the offset approach typically used.
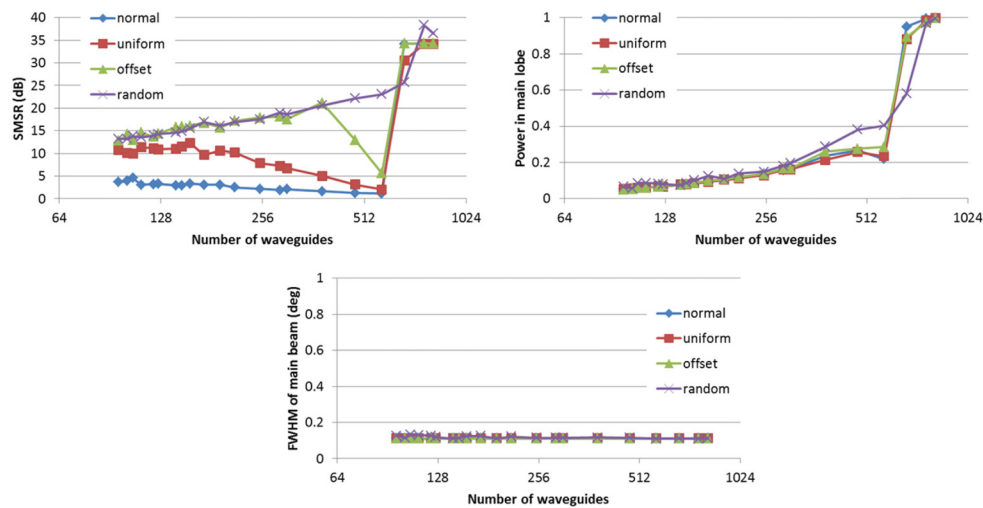

Fig. 8. SMSR, power in main lobe and FWHM of the main lobe as a function of number of waveguides for different randomization approaches of non-uniform OPAs.
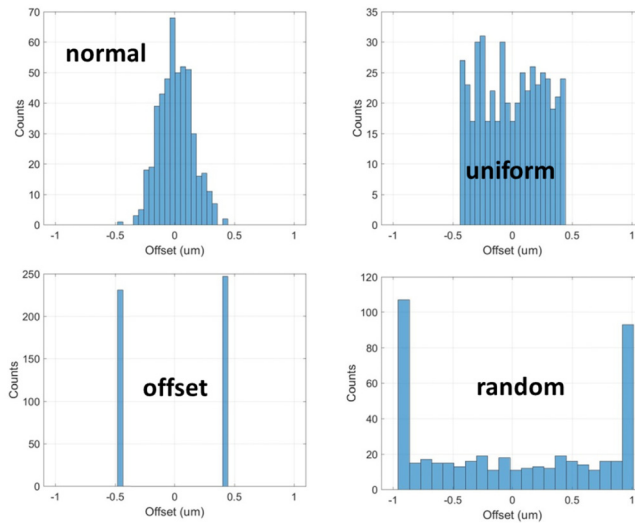
Fig. 9. Histograms showing typical offsets from the uniform pitch for the case of 480 waveguides for 4 considered randomization approaches. Minimum pitch is 1.2 μm in all cases.

Next we study the influence of minimum pitch as a function of number of waveguides for a 1 mm wide emitter using fully random waveguide placement. We consider five different minimum pitch values from sub-wavelength 1.2 μm to 3.5 μm (~2.25 λ) and show the results in Fig. 10. The SMSR generally improves as the number of waveguides is increased, until the minimum pitch limitation prevents the optimizer to arrange the waveguides so that the grating lobes are suppressed.
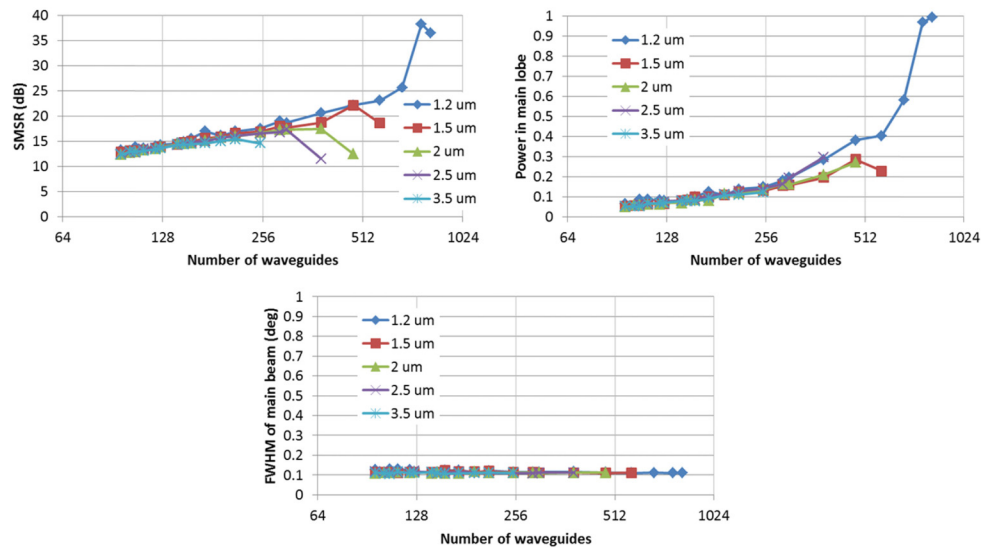
Fig. 10. Minimum pitch influence on SMSR, power in main lobe and FWHM of the main lobe as a function of the number of waveguides. The minimum pitch places a limitation on number of waveguides that can be placed with sufficiently random pitch in 1 mm area to suppress grating lobes. Besides that, there is little influence of minimum pitch on OPA performance.

For 3.5 μm minimum pitch, this happens between 212 and 252 waveguides, while for 2 μm pitch, the transition is around 302 waveguides. This clearly shows that fully random

waveguide placement allows for large waveguide separation where crosstalk does not present a problem. Due to randomized placement, the beamwidth is preserved and is equal to approximately 0.11°. It is slightly larger than the diffraction limit due to, already mentioned, the 10 dB excitation taper used to suppress sidelobes.

We select the 2.5 µm pitch, 192 waveguide case to study the steering performance. The array that was optimized at broadside (0° steering) shows relatively large variation in SMSR of ~4 dB when steered between broadside and 81° as shown in Fig. 11. We further compare the steering performance for arrays that were optimized at different angles of 12°, 35° and 65°, and show that a lower variation in performance can be obtained by optimizing the array at larger angles. The array optimized at 65° has variation of less than 1 dB, at the expense of somewhat lower SMSR close to the broadside. The effect on power in main lobe and FWHM is negligible. This shows that the randomized OPAs can be optimized depending on the FOV required.
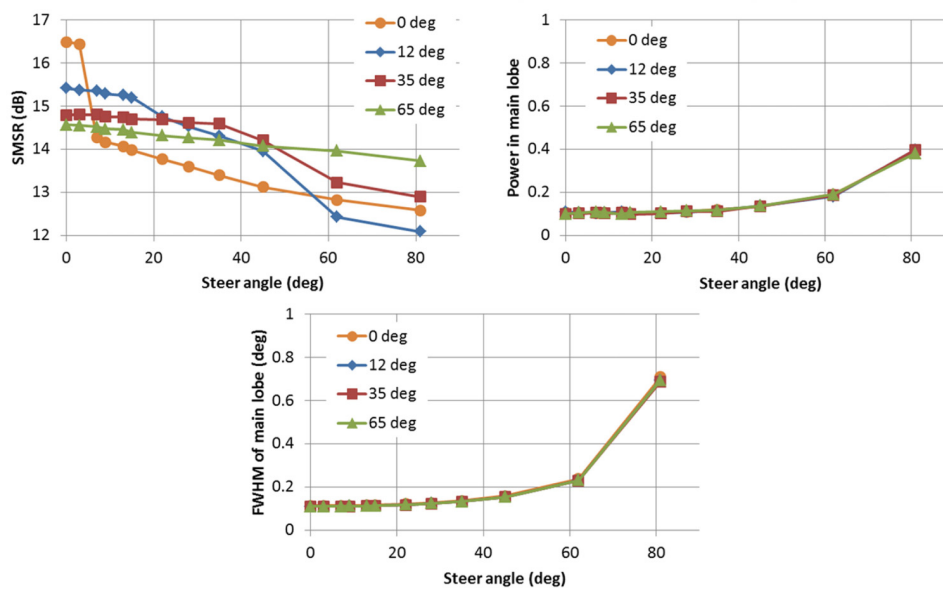

Fig. 11. Beam steering performance of randomized 192 waveguide OPA where the waveguide placement was optimized at broadside (0°) or at an angle (12°, 35° and 65°). Optimization at broadside results with higher SMSR at broadside, but also with larger SMSR variation as the beam is steered. Optimization of waveguide locations at larger angles reduces the SMSR at broadside, but lowers the SMSR variation as the beam is steered. Influence on power in main lobe and FWHM is negligible. The minimum pitch is 2.5 µm.

Due to allowing for larger spacing between the waveguides without sidelobes, randomized spacing, similarly to linearly changing pitch in Section 3.1, allows for wider elementary emitter which can reduce the power in sidelobes or, in other words, increase the relative power in the main beam. This increase in power of the main beam has a tradeoff in reduced scanning angle due to the higher directivity of the elementary emitters. In previous simulations, we have assumed that the elementary emitter has a Gaussian profile with 10 dB taper at ± 250 nm (500 nm total width). Now we show performance when the elementary emitter width is increased to 1 µm and 1.5 µm for the same 192 waveguide case, keeping the same Gaussian approximation. A more rigorous analysis would simulate the mode shape in the waveguide, but we keep the Gaussian approximation due to simplicity and number of degrees of freedom in designing the waveguide (Si device layer thickness, etch depth). The waveguide placement has been optimized for broadside emission. The results are plotted in Fig. 12, and show that by using a wider emitter, it is possible to considerably increase power

in the main beam, provided that the required FOV is limited. This allows further optimization of the OPA performance depending on the required FOV.
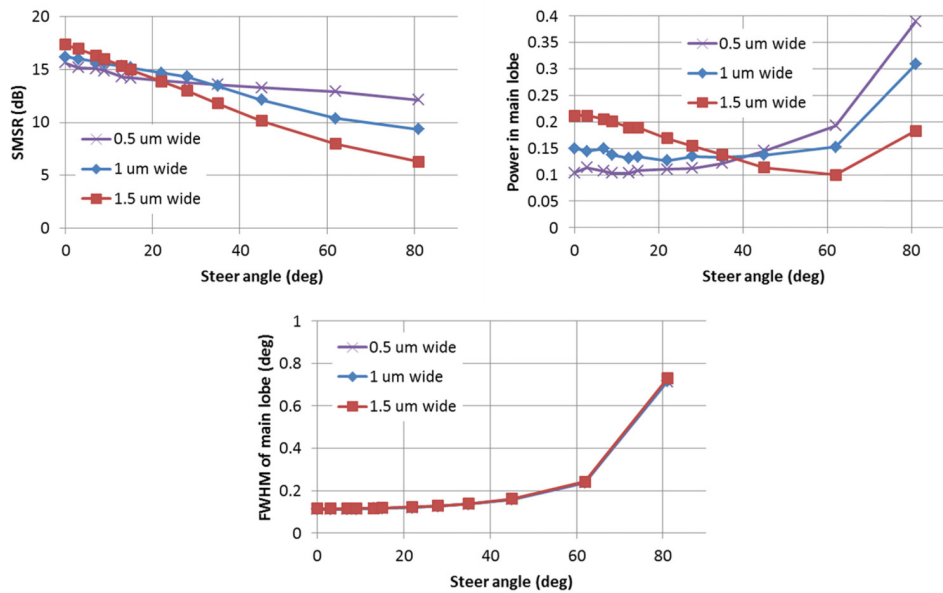

Fig. 12. Beam steering performance of randomized 192 waveguide OPA with 2.5 μm minimum pitch with different widths of elementary emitters. Using wider elementary emitter increases the power in main lobe if OPA FOV is limited.

4. Optimal OPA with reduced number of waveguides

We now directly compare the performance of 192 and 480 waveguide OPAs with linearly varying and fully random pitch. We select these two configurations to show the performance where cross-coupling stops being a critical issue (480 waveguides, average spacing 2.08 μm, minimum spacing 1.2 μm) and with much reduced number of waveguides compared to the uniform pitch with no grating lobes in visible space, which should allow much simpler contacts to the phase shifters and driving circuitry (192 waveguides, average spacing 5.2 μm, minimum pitch 2.5 μm). We show the comparison in Fig. 13.

For the 192 waveguide case, the PSO optimized array, compared to the linear change of pitch, can provide higher SMSR in whole visible space or much more uniform SMSR in the whole visible space (with somewhat lower SMSR very close to broadside) depending on the optimization angle for waveguide placement as addressed in Section 3.2. At the same time, it has a narrower main lobe (0.11° vs. 0.14°) leading to larger number of resolvable spots, but as a downside has lower power in the main lobe. The power is lower due to much higher quality of the beam as shown in Fig. 14.

We also plot the far-field patterns in full visible region for 192 waveguide configuration in Fig. 15, showing comparison between PSO optimized, linear and cubic waveguide placement at broadside and when steered to 65°. This far-field pattern can directly be compared with the far-field pattern of a uniform array with identical number of waveguides shown in Fig. 2(d). In all cases the minimum pitch is 2.5 μm.

The differences between the two approaches are much smaller for the case of 480 waveguides, with the exception of the PSO optimized for broadside, which has higher SMSR at broadside, but much worse SMSR when steered. The linearly changed pitch once again has higher power in main lobe with somewhat wider main lobe (0.13° vs. 0.11°), but with significantly improved quality of the main beam compared to 192 waveguide case.
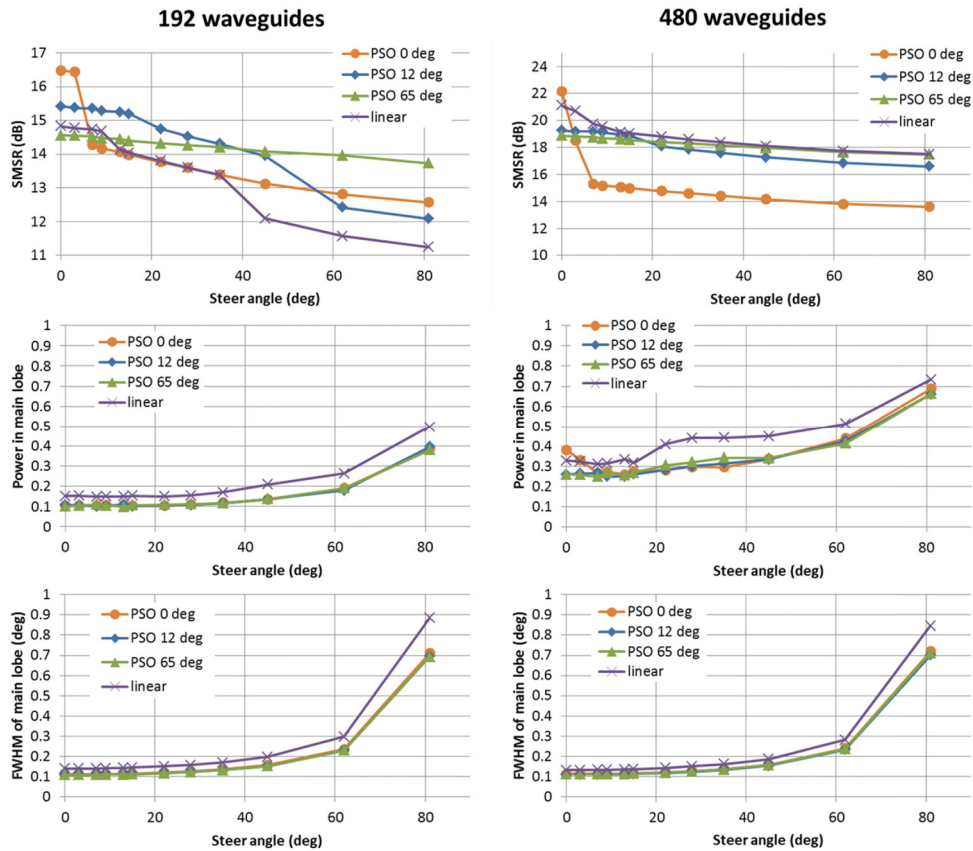
Fig. 13. Direct comparison in beam steering performance of 192 and 480 waveguide OPAs with randomized and linearly changing waveguide spacing. The minimum pitch is 2.5 μm and 1.2 μm for 192 and 480 waveguide case respectively.
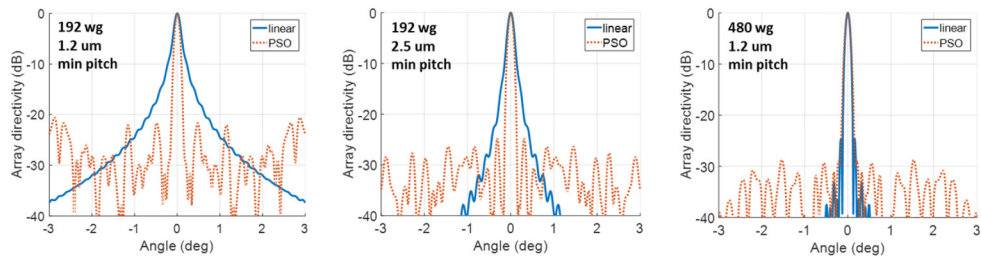

Fig. 14. Quality of the main beam for linearly changing and PSO optimized pitch for 192 waveguide configuration with two minimum pitch spacings (1.2 μm and 2.5 μm) and 480 waveguide configuration (1.2 μm minimum pitch). At lower waveguide counts, the linearly changing pitch sacrifices the quality of the main beam to suppress the sidelobes. The wider main lobe leads to higher ratio of power in the main lobe. At larger waveguide counts, the main beams are almost identical in shape.

Finally, we study the influence of the operating wavelength to the phase steering performance of the OPA. We take the optimized 192 waveguide (PSO) and 480 waveguide (linear chirp) configurations and calculate SMSR in wide wavelength range of 300 nm around 1550 nm, which corresponds to approximately 45° of steering in the wavelength direction. Even in such a large wavelength range, the performance of the OPA is largely insensitive to

wavelength with <1.5 dB variation for 192 waveguide case and <4 dB variation for 480 waveguide case (Fig. 16).

As a conclusion, at lower waveguide counts, the PSO optimized spacing is preferred, while at medium waveguide counts, both the PSO optimized and linearly changing pitch offer similar performance levels.
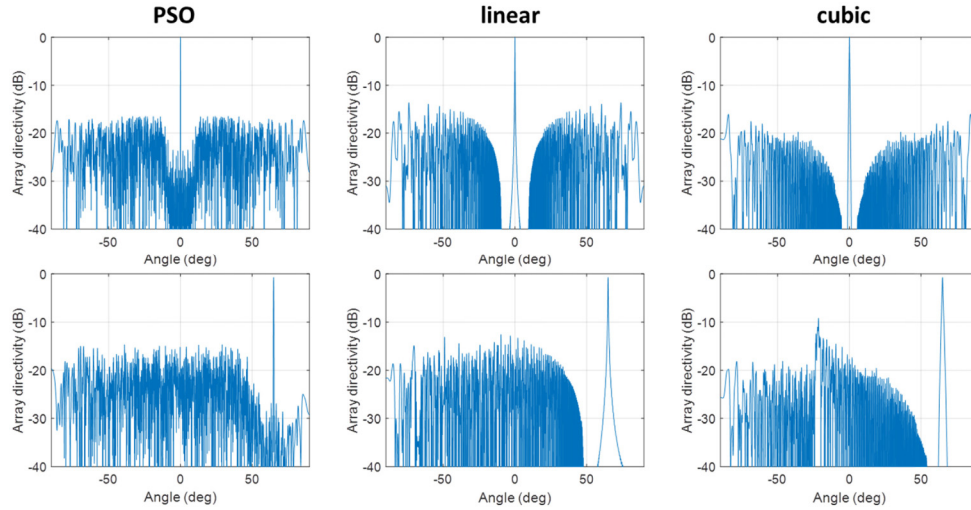

Fig. 15. Illustrative far-field patterns for an array with 192 elements when pointing at broadside (top row) or when steered to 65° (bottom row) for PSO optimized, linear and cubic waveguide placement strategies. In all cases grating lobes are significantly suppressed compared to the uniform array shown in Fig. 2(d).
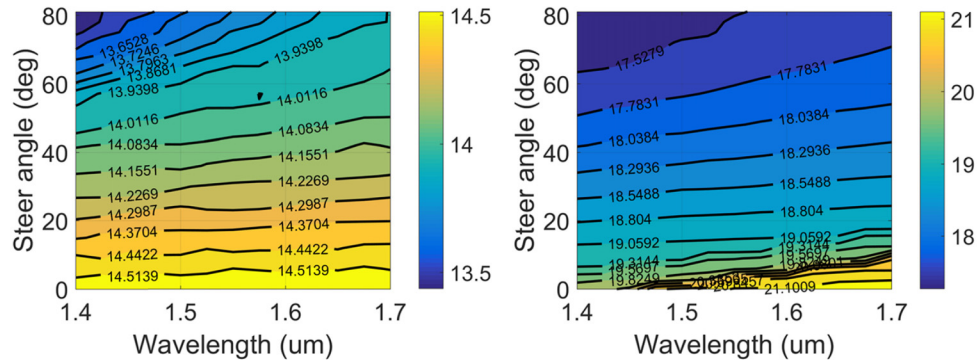

Fig. 16. SMSR as the OPA is steered in both directions using wavelength and phase tuning. (left) 192 waveguides, PSO optimized, 2.5 μm minimum pitch, optimized at 65° (right) 480 waveguides, linearly changing pitch, 1.2 μm minimum pitch

4.1 Scaling to larger areas

Due to the number of elements and the size of the chips considered, it is reasonable to assume that for even larger arrays in cm scale, smaller cells (e.g. 1 mm as considered here) and tiling could be used. This approach is also known as "sub-phased arrays". Tiling allows for prescreening of individual cells and potentially higher yields of large OPAs. One could envision a number of different cell elements that are optimized to work as a larger array, but that introduces some restrictions and complicates the process. Ideally there would be one basic cell that can then be tiled as needed. Here we study the performance of linearly changing pitch and PSO optimized pitch cells when tiled. We take the 192 waveguide array

with 2.5 μm minimum pitch as shown in Section 4 as a unit cell and then stitch them together to increase the size of the emitter area to 5 and 10 mm. We show results in Fig. 17, where we compare them to a larger single cell OPA (10 mm in size, 1920 waveguides, 2.5 μm pitch). Stitched PSO optimized OPAs have the same beam width and power in the main lobe as single cell larger OPAs, but have lower SMSR as waveguide positions are not optimized optimally to suppress grating lobes in all directions. In case of the linear arrays, stitched ones have narrower main lobe resulting with somewhat lower power in the main beam and also have lower SMSR as grating lobes are not suppressed to the extent they are with larger single cell OPAs. As a conclusion, preliminary stitching studies show that larger unit cells can provide improved SMSR compared to smaller ones. In other words, there is a penalty associated with using identical smaller cells when building larger OPA by tiling in terms of SMSR, but depending on the yield, that might be a reasonable tradeoff as power in main lobe and beamwidth are largely unaffected. An alternative approach for increasing the yield of large devices was studied in [29].
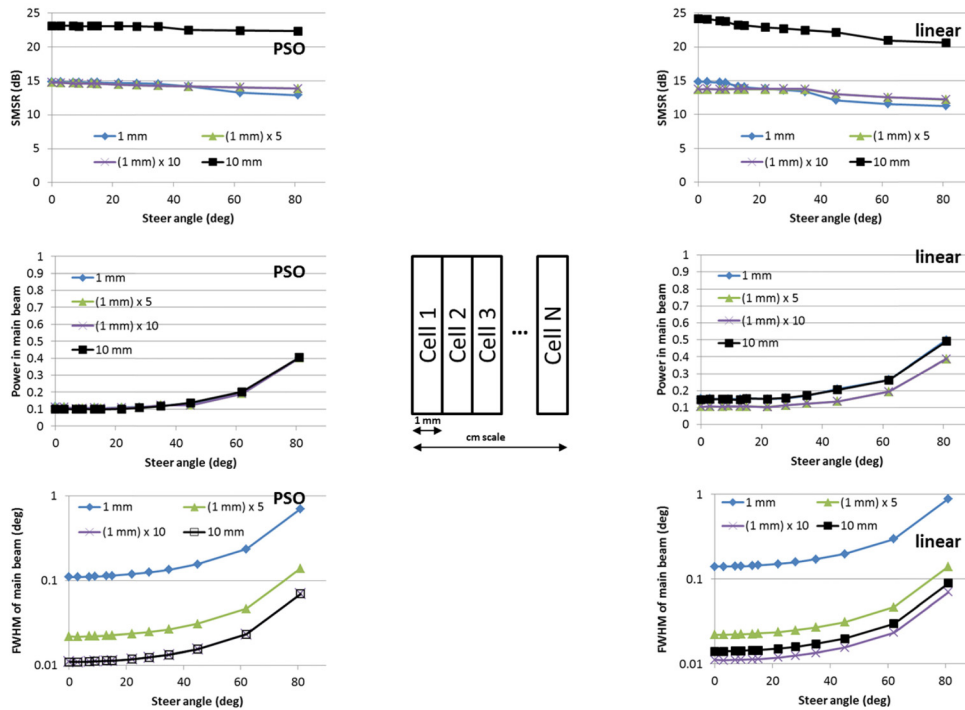

Fig. 17. Performance of stitched 1 mm unit cells with 192 waveguides and 2.5 μm minimum pitch compared to large 10 mm single cell array. (left column) PSO optimized cell (right column) cell with linear change of pitch (middle) inset showing the stitching strategy.

5. Conclusions

We analyze sparse aperiodic arrays for optical phase steering and LIDAR applications and show that, e.g. 192 element array can provide grating lobe free steering in whole visible space ($\pm$ 90°) with decent > 13.5 dB SMSR using > 3 λ average spacing between elements. This allows for more than six times reduction in number of elements compared to uniformly spaced array, reducing the cost, complexity and improving the yield while keeping the same beam width and same number of resolvable spots in the far-field. Furthermore, the minimum pitch can be larger than > 1.5 λ, removing the cross-coupling issues completely, provided that the optical phased array is realized in a high-index contrast waveguide platform (such as Si/SiO_2).

We show that for best performance, a global search optimization and a fully-random strategy should be utilized, at least at low waveguide densities (> 3 λ average spacing). Furthermore, we demonstrate that for more uniform steer performance, it is beneficial to optimize the array placement at an angle initially.

For medium waveguide densities (~1.5 λ average spacing) ordered non-uniform waveguide spacing can be used due to simplicity and similar performance to the PSO optimized one. In that case, for a wide field of view, a linear change in spacing between the elements seems to be optimal.

Finally, we show ways to improve array performance if a reduced field of view is acceptable and consider stitching multiple smaller cells for scaling to larger emitter areas in order to improve yield.

6. Funding

Acknowledgments